Reactivity of 12-tungstophosphoric acid and its inhibitor potency toward Na + /K + -ATPase: A combined 31 P NMR study, ab initio calculations and crystallographic analysis

Nada Bošnjaković-Pavlović, Danica Bajuk-Bogdanović, Joanna Zakrzewska, Zeyin Yan, Ivanka Holclajtner-Antunović, Jean-Michel Gillet, Anne Spasojević-de Biré

Reactivity of 12-tungstophosphoric acid and its inhibitor potency toward Na^+/K^+-ATPase: a combined ^{31}P *NMR* study, *ab initio* calculations and crystallographic analysis

Nada Bošnjaković-Pavlović[a*], Danica Bajuk-Bogdanović[a], Joanna Zakrzewska[b], Zeyin Yan[c,d], Ivanka Holclajtner-Antunović[a], Jean-Michel Gillet[c,d] and Anne Spasojević-de Biré[c,d*]

[a] Faculty of Physical Chemistry, University of Belgrade, P.O. Box 47, 11001 Belgrade, Serbia

[b] Institute of General and Physical Chemistry, Belgrade, Serbia

[c] Université Paris-Saclay, CentraleSupélec, Campus de Châtenay, Grande Voie des Vignes, 92295 Châtenay-Malabry, France

[d] CNRS, UMR 8580, Laboratory "Structures Propriétés et Modélisation des Solides" (SPMS), Grande Voie des Vignes, 92295 Châtenay-Malabry, France

authors to whom correspondence should be addressed

nadab@ffh.bg.ac.rs

anne.spasojevic@centralesupelec.fr

to be submitted to Journal of Inorganic Biochemistry

Abstract

Influence of 12-tungstophosphoric acid (WPA) on conversion of adenosine triphosphate (ATP) to adenosine diphosphate (ADP) in the presence of Na^+/K^+-ATPase was monitored by ^{31}P NMR spectroscopy. It was shown that WPA exhibits inhibitory effect on Na^+/K^+-ATPase activity. In order to study WPA reactivity and intermolecular interactions between WPA oxygen atoms and different proton donor types (D = O, N, C), we have considered data for WPA based compounds from the Cambridge Structural Database (CSD), the Crystallographic Open Database (COD) and the Inorganic Crystal Structure Database (ICSD). Binding properties of Keggin's anion in biological systems are illustrated using Protein Data Bank (PDB). This work constitutes the first determination of theoretical Bader charges on polyoxotungstate compound *via* the Atom In Molecule theory. An analysis of electrostatic potential maps at the molecular surfaceand charge of WPA, resulting from DFT calculations,suggests that the preferred protonation site corresponds to WPA bridging oxygen. These results enlightened WPA chemical reactivity and its potential biological applications such as the inhibition of the ATPase activity.

Graphical abstract

In order to analyze the reactivity of 12-tungstophosphoric acid (WPA), DFT calculations have been performed and the consequent electrostatic potential values at the molecular surface of Keggin anion have been determined.The results of ^{31}P NMR spectroscopy confirm that WPA exhibits inhibitory effect on the activity of Na+/K+-ATPase.

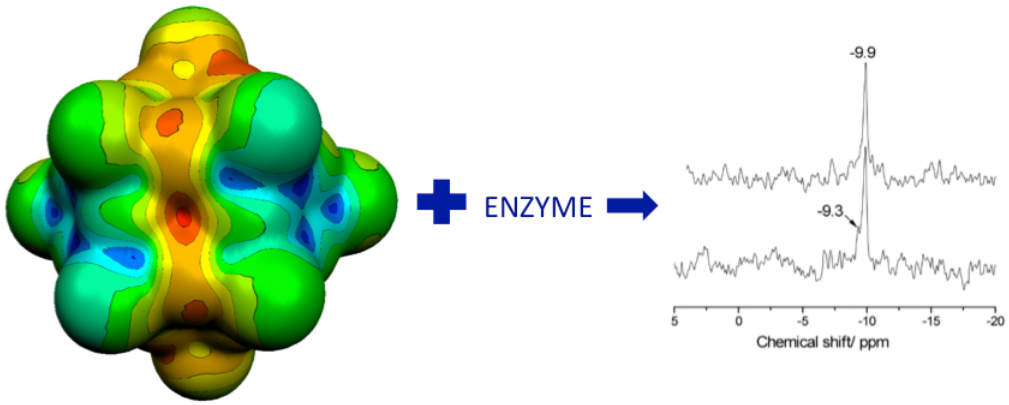

Highlights

• ^{31}P NMR shows that ATP hydrolysis is inhibited by WPA.

• Terminal oxygen atoms give stronger non covalent interactions than bridging oxygen atoms in the solid state.

• *Ab initio* calculations indicates that the most nucleophilic sites are the bridging oxygen atoms.

Keywords: Polyoxometalates, 12-tungstophosphoric acid, Na^+/K^+-ATPase, ^{31}P nuclear magnetic resonance, density functional theory, Cambridge Structural Data Base analysis

1. Introduction

Polyoxometalates (POMs) are a class of metal-oxygen cluster compounds with unique structural and physicochemical properties [1].They have attracted great attention for many years due to their strong acidity and redox properties, which have lead to their broad applications in industry as homogeneous and heterogeneous catalysts [2-5]. POMs are generally nontoxic to normal cells and exhibit *in vitro*,and *in vivo* biological activities [1, 6-10]. Such activities include highly selective inhibition of enzyme functions, *in vitro* and *in vivo* antitumoral [11-15], antiviral [16] and antiretroviral activities [17] against human immunodeficiency virus (HIV) infections.

Biomedical importance of POMs, as confirmed by numerous studies is mostly based on their interactions with proteins [10, 14, 18-21]. These studies illustrate the importance of noncovalent interactions between POM and peptides. Negative charge of POMs is thought to be one of the key features for their interactions with proteins, as POMs are binding primarily to the positively charged protein region [22]. It is consistent with the experimental results obtained by Zhang *et al.* indicating that the binding of POM to proteins may cause the protein molecule to undergo an unfolding process [23].

Among the POMs, 12-tungstophosphoric acid ($H_3PW_{12}O_{40}$ abbreviated WPA) occupies a special position. It is recognized as a promising catalyst in biomass fuel production [24-25]. The anion has also various biological properties [26-33], including inhibition of ATPase.Primary structure of WPA is the Keggin unit, which is composed of a central PO_4^{3-} tetrahedron surrounded by 12 WO_6 octahedra as a polyanion $(PW_{12}O_{40})^{3-}$ with three negative charges that are neutralized by three protons. Figure 1 represents the anion structure. According to a representation of oxygen octahedron (Figure 1b), 4 oxygen types can be defined; 4 central oxygen atoms (Oa), 12 oxygen atoms that bridge two tungsten

atoms sharing a central oxygen atom (edge-sharing Oc), 12 oxygen atoms that bridge tungsten atoms not sharing a central oxygen atom (Ob) and 12 terminal oxygen atoms (Od) bound to a single tungsten atom. However, a precise analysis of the WPA geometry shows that there is no significant difference (as deduced from classical X-ray diffraction) between Ob and Oc oxygen atoms in terms of bond lengths and bond angles. It remains than in solution the accessibility of the Ob and Oc oxygen atoms could be distinguished as demonstrated by Lopez et al *via* molecular dynamic simulations [34]. Therefore, two types of "external" oxygen atoms, those which are accessible to a noncovalent interaction, will be used, according to their tungsten coordination: O1x (bonded to only one tungsten atom) and O2x (shared between two tungsten atoms). They will be referred to as O1 and O2 in this paper (Figure 1a).Oxygen atoms of a WPA anion are attractive sites, and can therefore form intermolecular hydrogen bonds. These interactions bear a particular importance because they are responsible for their biological actions towards viral enzymes or viral cell envelopes.

Precise proton positions and acid strength of tungstophosphoric acid, which are essential for understanding of the nature of the catalytic sites and reactivity, are still under active debate in the community. Kozhevnikov *et al.* [35] concluded from ^{17}O NMR spectroscopy that the protons are located on the terminal oxygen atoms (O1). Ganapathy *et al.*[36] reached a similar conclusion based on the results from $^{1}H/^{31}P$ and $^{31}P/^{1}H$ Rotational Echo Double Resonance (REDOR) NMR experiments and density functional theory (DFT) based quantum chemical calculations of the proton affinity for a single proton. ^{31}P NMR analysis and DFT calculations indicated that the trimethylphosphine oxide complexes are associated with protons located at three different terminal oxygen (O1) sites of the WPA polyanion [37]. Solid-state NMR technique [38] was used to argue that the anhydrous protons reside on the bridging oxygen atoms. The most energetically favorable site for the

acidic proton in anhydrous heteropolyacids was determined by quantum chemical calculations to be a bridging oxygen atom [39]. DFT calculations, which considered the position of all three protons, indicated that the energy preference for either oxygen type is small and that protons are likely to be distributed among all oxygen types [40].REDOR NMR experiments combined with quantum chemical DFT calculations demonstrated that acidic protons in anhydrous WPA are localized on both bridging (O2) and terminal (O1) atoms of the Keggin unit[41].

Recently, we found that WPA exhibits potential bioactivities, especially the inhibition of Na^+/K^+-ATPase [31]. In a number of enzyme reactions involving phosphates, the most direct method for monitoring interaction between WPA and enzyme and identification of generated chemical species is ^{31}P NMR spectroscopy [42-44]. The possibility of readily distinguishing and assigning each phosphorus atom of adenosine triphosphate (ATP) and adenosine diphosphate (ADP) by ^{31}P NMR was early recognized and demonstrated in 1960 [45]. Therefore we applied ^{31}P NMR to follow ATPase activity in the presence of WPA.

The understanding of the interaction, between WPA and enzyme (ATPase), at a molecular level is essential for the interpretation and the development of potent compounds with selective enzymatic affinity. In order to understand the reactivity of WPA, the OH···O, NH···O and CH···O interactions between different organic parts and WPA were analyzed using the Cambridge Structural Data Base (CSD) [46], Crystallographic Open Database (COD) [47] as well as the Inorganic Crystal Structure Database (ICSD) [48] or the Protein Data Bank (PDB) [49]. This analysis was performed according to the oxygen atom type (O1 or O2). Consequently, it explains the interaction of organic molecules with Keggin anion through hydrogen bonding. Hydrogen bonds, weak interactions and their environment have a well–documented geometry in the crystalline state. CSD provides a large amount of experimental data that allows a betterdescription of

hydrogen bonds geometry [50-53]. This method has already been applied to different POMs compounds such as decavanadate [54] and functionalized hexavanadate [55].

The aim of this paper is a contribution to a better understanding of the WPA anion reactivity and its inhibitor potency toward Na^+/K^+-ATPase. These interactions have been studied through a combined approach using both theoretical and experimental tools. We have investigated the action of the ATPase inhibitor WPA on the breakdown of extracellular ATP. The influence of WPA binding to Na^+/K^+-ATPase activity in conversion of ATP to ADP is supported by an analysis of ^{31}P NMR spectroscopy data. To achieve this goal, a theoretical analysis of various interactions of WPA, has been provided, with an emphasis on the changes of bonding nature depending on the oxygen position in the molecules (O1 or O2). Binding properties of Keggin anion in a biological system are illustrated using the PDB.A more efficient and elegant method to predict ligand binding sites involves the use of DFT calculations and the subsequent determination of the electrostatic potential (EP) values at the molecular surface of WPA.

2. Materials and methods

2.1. Chemicals

All chemicals were of analytical grade. Na^+/K^+-ATPase from porcine cerebral cortex and ATP were purchased from Sigma Chemicals Co. (Germany), as well as some chemicals for assay medium (magnesium chloride and Tris–HCl). WPA was prepared according to the literature [56] and the structure confirmed by powder X-ray diffraction and infrared spectroscopy. Synthesized WPA was recrystallized prior to use and heated about 10 minutes at 80 ^{o}C in order to get stable acid hexahydrate ($WPA{\cdot}6H_2O$).

2.2. Medium for ^{31}P NMR experiment

The standard assay medium for common investigation of Na^+/K^+-ATPase activity was used in our ^{31}P NMR experiment.The mediumcontained (in mmol/L): 50 Tris–HCl (pH 7.4), 100 NaCl, 20 KCl, 5 $MgCl_2$, 2 ATP and 125 mgL^{-1} SPM proteins (i.e. 290 mgL^{-1} commercial porcine cerebral cortex proteins) in a final volume of 5 ml. After preincubation for 10 min at 37 °C in the absence (referred hereafter as control solution) or in the presence (referred hereafter as probe solution) of investigated WPA compound, the reaction was initiated by addition of ATP. Concentration of WPA in the probe solution was $1 \cdot 10^{-3}$ $moldm^{-3}$.Probe solution pH was measured using a pH meter with a glass electrode and adjusted by addition of NaOH up to pH 7.4.Blank solution was prepared without addition of enzyme and WPA.

2.3. ^{31}P NMR spectroscopy

NMR experiments were carried out on Apollo upgrade (Tecmag, USA) Bruker, MSL 400 spectrometer, at 161.978 MHz, with 2048 scans, 9.0 μs pulse and 500 ms repetition time, at 25 °C. ^{31}P NMR spectra of control solution (ATP, enzyme), and probe solution containing WPA were recorded in different time intervals: immediately, 4 h, and 4 days after addition of ATP. The duration of spectra recordings was 20 min. In the meantime solutions were kept at 4 °C. 85% H_3PO_4 at 0 ppm was used as external standard for the chemical shift estimation.

2.4. Structural searches

2.4.1. Cambridge Structural Data base (CSD)

CSD was searched for compound containing WPA anion and retrieved depending on the oxygen type O1 and O2 (see supporting information, Table S1). The searches were restricted to entries with: a) error-free coordinate sets in CSD check procedures; b) no crystallographic disorder; c) no polymeric connections and d) crystallographic R factor

lower than 0.10. For each interaction, D-H···O distance (D as donor atom) and D-H···O angle using Mercury® software[57] are shorter than the sum of their van der Walls radii.

2.4.2. Crystallographic Open Database (COD)

COD [47] was searched for compound containing WPA anion and retrieved depending on the oxygen type O1 and O2 (see supporting information, Table S2). The searches were restricted to entries with: a) no crystallographic disorder; b) no polymeric connections and c) crystallographic R factor lower than 0.10. For each interaction, D-H···O distance (D as donor atom) and D-H···O angle using Mercury® software[57] are shorter than the sum of their van der Walls radii.

2.4.3. Inorganic Crystal Structure Database (ICSD)

ICSD was searched for compound containing WPA anion. A similar methodology to those explained in section §2.4 and 2.5 has been used to determine the geometry of the structures found (see supporting information, Table S3).

2.4.4. Protein Data Bank (PDB)

PDB was searched for WPA···H-donor interactions. The enzyme–WPA complexes were found through a PDB search using the “Keggin anion” or “tungstophosphoric” keyword leading to 3 structures (see supporting information, Table S4). Geometry of intermolecular interactions between the Keggin anion and the protein structure were determined.

2.5. *Ab initio* computations

All *ab initio* computations have been carried out with Gaussian09 package [58]. These calculations were based on B3LYP hybrid functional, which uses a combination of the Becke exchange functional [59] coupled with the correlational functional proposed by Lee *et al.* [60, 61]. The triple-ς and polarization type basis set cc-PVTZ [62] was chosen for phosphorus, oxygen, nitrogen, carbon and hydrogen. As for tungsten atom, the

effective core potential type basis set LANL2DZ [63] was used to limit computational effort, while the Douglas-Kroll-Hess [64, 65] second order scalar relativistic calculation was used to account for relativistic effects at moderate cost. MultiWFN package [66] based on Bader's Atoms in Molecules Theory (AIM) has been used to define atomic basins and their integrated charges. Since an effective core potential was chosen to describe part of W atoms. Non-nuclear attractors [67] were found in the immediate vicinity of W nucleus and need to be back integrated into the nearest W basin contribution.

3. Results and discussion

3.1. Inhibition of ATPase followed by ^{31}P NMR spectroscopy

As shown in our earlier study WPA exhibits concentration-dependent inhibitory effect on the activity of rat synaptic plasma membrane Na^+/K^+-ATPase and E-NTPDase [31].The behavior of WPA in solution is important from the aspect of analytical, biomedical, and catalytic applications. Analysis of Fourier transform infrared (FTIR) and Raman spectra have has shown that WPA in the incubation medium i.e. in the presence of commercial enzyme and its substrate-ATP, forms monolacunary Keggin anion $[PW_{11}O_{39}]^{7-}$ as the main molecular species in the system under physiological conditions [31, 68-69]. This species arises by removal of one WO unit from the Keggin anion and may reacts with various ligands, including Na/K ATPase, responsible for ATP hydrolysis. In this paper we wanted to follow the changes in molecular structure of heteropoly acid WPA applying ^{31}P NMR spectrometry as a common method for analyzing of heteropoly acids of Keggin structure as well as their hydrolysis molecular products. Simultaneously this method enables a direct observation of the enzyme interaction, like the ATPase, with the chemical moieties that actually participate in the reaction [70].

Figure 2 contains ^{31}P NMR spectra of blank (left), control (middle) and probe (right) solutions, recorded at different time intervals: immediately(a), 4 h (b), and 4 days (c) after solution preparation.Assignments of the signals can be readily made on the basis of known ^{31}P NMR spectra of ATP and ADP [45]. Three ATP peaks (α -9.8 ppm, β -18.2 ppm; and γ -4.6 ppm) are clearly visible in the ^{31}P NMR spectra of the control, and the probe solutions recorded immediately after preparation. However, in the control spectrum recorded 4 hours after preparation, two additional small peaks, superimposed on α, and γ ATP peaks are observed at -9.2 ppm and -5.0 ppm, originating from α ADP and β ADP respectively. These peaks are indicating the beginning of ATP hydrolysis. The peak of released inorganic phosphate Pi, at +3.2 ppm is also visible. These changes were more expressed in the spectrum recorded after 4 days. The intensity of Pi signal is considerably enhanced, and a weak peak at +4.6 ppm is observed at expected position for AMP as a result of ATP hydrolysis and formed ADP [71]. The appearance of the spectra in Figure 2 (middle) may be explained by irreversible ATP hydrolysis, i.e. the ATP concentration is progressively reduced while the concentration of ADP, AMP and Pi is increased.

On the other hand, no changes are observed in ATP signals when WPA is present (probe solution, Figure 2, right). Therefore, the signal of β-ATP, as the signal belonging solely to ATP molecule [72] was used for estimation of changes in ATP content. We have compared its normalized area in the blank, control and probe sample in different time intervals. The results are presented in Figure 3 and indicate that ATP content in control solution was reduced for about 40% four days after preparation of solution. No changes of ATP level was detected in the presence of WPA in the same time interval.

As shown in our earlier study [31], WPA in the presence of commercial enzyme and its substrate-ATP forms monolacunary Keggin anion $[PW_{11}O_{39}]^{7-}$, the main molecular species, which is proved to be the active species in aqueous solution at physiological

pH.The ^{31}P NMR spectrum of WPA in the incubation medium without ATP and ATPase is presented in Figure 4a. The dominant peak at about -9.9 ppm, corresponding the monolacunary Keggin anion present under physiological pH [68], is not observed in the spectra presented in Figure 2 because of low WPA concentration and overlapping of its signal with more intensive peak of α-ATP. Therefore in this way we could not follow the changes in molecular structure of WPA during ATP hydrolysis. However in the experiment where only WPA and enzyme (without ATP) were present under the same experimental conditions, changes in the ^{31}P NMR spectrum (broadening of signal at -9.9 ppm and appearance of shoulder/peak at -9.3 ppm) could be an indication of interaction of enzyme and a monolacunary WPA anion(Figure 4b).

In order to get further insight about the understanding of the interaction WPA – enzyme, these interactions existing in solution state are studied *via* a crystallographic statistical study (section 3.2 and 3.3) in solid state and *via* the determination of the atomic net charges, electrostatic potential on the WPAmolecular surface in gas state (section 3.4).

3.2. Geometrical description of WPA interactions with organic moieties in crystalline state

Statistical study on the O-H···O, N-H···O and C-H···O non-covalent interactions for 36 structures containing Keggin anion (WPA) found in CSD [S1], COD [S2], ICSD [S3] and PDB [S4] databases (Table 1), have been performed.160 contacts have been identified: 23 O-H···O interactions, 2 N-H···O and 135 C-H···O interactions. These interactions were sorted according to the oxygen type of WPA (O1 and O2). Figure 5 represents D-H…O angles *versus* H···O distances distribution containing inorganic compound or hybride organic-inorganic compound retrieved from ICSD, when D···O distances are less than 3.5 Å. The O···H distances show an accumulation between 1.7 and 2.4 Å while the O-H···O angle exhibits values between 125 and 175 ° (Figure 5, squares).One can observe

twoaccumulations of O-H···O interactions: a strong one (from 1.7 to 2.0 Å, at higher angles) and a weaker one (from 2.1 to 2.5 Å, at smaller angles).Geometry of 24 C-H···O interactions is analyzed using interactions from 13 crystal structures (triangles) from ISCD database and 111 interactions from 37 structures from CSD database (Figure 5, triangles and Figure 6, triangles). All these interactions follow the trend expected for hydrogen bonds, namely for C-H···O angle opens up as the distance between donor and acceptor increases. C-H···O interactions are mainly at long distance (2.4 to 2.8 Å) and the angles range from 110 to 160 °. In terms of angularity, all these interactions follow the trend expected for hydrogen bonds [73].O-H···O non-covalent interactions (Figure 6) for the oxygen O1 are mainly at a short distances (1.7 to 2.0 Å) and high angles (155 to 175 °) whereas for O2 the interactions are at longer distances (2.1 to 2.5 Å) and smaller angles (90 to 150 °). O1 oxygen atoms build the C-H···O interactions from 2.3 to 2.7 Å. For O2 these interactions are at longer distances (2.5 to 2.8 Å). It is therefore clear, that the directionality of the non-covalent interactions depends on the oxygen atom type. O1 oxygen atoms induce strong directionality for O-H···O interactions with short distances and high angle and O1 build stronger C-H···O interactions. O2 can form O-H···O but usually with very long distances (2.1 - 2.5 Å) and with smaller angles (100 to 140 °). In consequence, summation of all the interactions expressed by the 34 structures containing WPA anion clearly indicated than O1 atoms build significant more interactions than oxygen atoms O2 (129 interactions for O1 versus 83 for O2, Figure 7). Further more the distribution median is very slightly greater for O2 atom (2.574 Å) than for O1 atom (2.558 Å) indicating than the $CH\cdots O_{WPA}$ interactions with O1 atom could appear slightly stronger than the interactions with O2 atom.

3.3. Keggin anion binding with proteins

Čolović *et al*[31] have clearly demonstrated than WPA exhibits an inhibitory effect on the activity of rat synaptic plasma membrane Na^+/K^+-ATPase andthe ecto-nucleoside triphosphate diphosphohydrolase (E-NTPDase). Bijelić *et al*[10] have shown that almost all POMs are located at positively charged protein regions due to their negative charge and to their ability to form charge–charge interactions and hydrogen bonds. The relatively high content of polar residues indicates a high contribution of hydrogen bonds in POM-binding since almost all polar uncharged side chains have one hydrogen donor atom [10]. Biological activities could be related to ionic size and shape, electron- and proton- transfer ability, reservoir properties (i.e. inhibition of biological electron transfer) and stability at micromolar concentration and physiological pH [10]. PDB database was searched for protein structures with Keggin anion, in order to investigate their interactions with WPA and possible impact on the protein structure, which might have influenced the crystallization process. Therefore, the ligand search engine from the PDB was utilized and we searched for commonly used transition metals that were reported to act as addenda atoms in POMs (Mo, V and W). Three Keggin structures, for which the coordinates are available, have been retrieved from PDB (as of January 2017), Table 1:low-density lipoprotein receptor (**1n7d**) [S4a], protein phosphotase (**2hhl**) [S4b] and Saccharomyces cerevesiae (**5suq**) [S4c]. Table 2 summarizes the intermolecular interactions between Keggin anion and the rest of the structure, in these three proteins.WPAis bound with serine, arginine molecules and asparagine in (**1n7d**). The contact $O1\cdots O_{Arg}$ with the distance O···O about 2.44 Å is the shortest contact, and can be assumed as a hydrogen bond.Keggin anion in (**2hhl**) is bound to lysine, histidine, serine and phenylalanine *via*hydrogen bond. Three different Keggin anion are linked to aspartic acid, threonine, lysine, arginine, asparagine in (**5suq)***via* hydrogen bond. In these three structures hydrogen bonds are formed between Keggin anion and polar (serine, asparagine, threonine), positive

charged amino acid (arginine, lysine, histidine), negative charged amino acid (aspartic acid) and uncharged acid like (alanine, phenylalanine).In all structures, a large number of interactions take place on the most reactive oxygen O1 atoms (22 interactions for O1 *versus* 9 for O2) leading to almost 70 % of hydrogen bonds are formed with O1 atoms.The results show that WPAs bind with the protein in the active site region withpositively charged protein regions *via* hydrogen bonds. Therefore, these results show that the WPAnon-covalent behavior deduced from the crystallographic statistical study based on WPA in interaction with organic molecules, remains the same when the anion is bounded to a protein.

3.4. *Ab initio* determination of the net atomic charges and the electrostatic potential

Different theoretical calculations using various approximations involving WPA^{3-} have been reported in the litterature. Acidity of WPA was the goal of several studies [3, 35, 39-41, 74-76]. The most energetically favorable site for the acidic proton in anhydrous heteropolyacids was determined by quantum chemical calculations to be a bridging oxygen atom [39]. The bridging oxygen atom between tungsten atoms that share a central oxygen atom (edge-sharing, O2) is the favored site for the addition of the first proton to the WPA^{3-} core [40]. Acidic protons are localized on both bridging (O2) and terminal (O1) oxygen atoms of the Keggin unit [41].

Ab initio calculations were used to ascertain the reactivity of oxygen atoms through the determination of the net atomic charge and the EP values on the molecular surface [54, 55]. EP can be used as a tool for predicting chemical reactivity, especially for non-covalent interactions. Guan *et al.* [77] suggest than the prefered proton site corresponds to a bridging atom (O2) and terminal oxygen (O1) after an observation of the EP mapped on the molecular surface in WPA^{3-}. Additionallly*ab initio* determination of spectroscopic data

[78-79], molecular dynamics[80] or docking studies [81, 82] have been performed with WPA as the target compound.

DFT functional types have been extensively studied by Wu *et al* [83]. The B3LYP functional chosen in this work gives satisfactoryresults according to the study of Wang *et al* [83]. Results of *ab initio* determination of the Bader net atomic charges are given in Table 3. The average value is used for atom W and O (12 W, 4 $O_{inner,}$ 12 O_1 and 24 O_2 in WPA^{3-}). These values are compared to those determined in the literature. This work constitutes the first determination of Bader charges on polyoxotungstate compound. As usually observed [84], Bader charges have greater amplitudes than those from a Mulliken scheme or the natural charges [36, 77, 78, 81]. In a previous work, we have experimentally determined the Bader charges of the polyoxovanadate $[V_{10}O_{28}]^{6-}$ [84] and compared to those determined by Henry *et al.* [85] (PACHA charges) and Kempf *et al.* [86] (Mulliken charges). It is interesting to notice that the difference (Δ) between the average charges of the bridged O2 atoms and the charge of the terminal O1 atom is approximately -0.2 (-0.23 for WPA^{3-} and -0.17 for $[V_{10}O_{28}]^{6-}$) (table 3, last line). The ChelpG atomic net charges obtained by Lopez *et al* [34] has not been used for the determination of this average difference due to the great difference with the other values. These results clearly indicate that the bridged O2 atoms are more acidic or are more reactive than the terminal O1 oxygen. These theoretical results are in agreement with the conclusions obtained by Bardin *et al* [40], Janik *et al* [41] and Yang *et al* [44] from theoreticalstudies based on other parameters than atomic charges.

Figure 8 represents three orientations the EP of WPA^{3-} mapped onto an 0.001 a.u. electron probability isodensity surface. EP values are the most negative (red) in the vicinity of bridged O2 atoms. This corresponds to the most nucleophilic regions, while the blue part (positive) is concentrated in the vicinty of the tungsten atoms and represents the most

electrophilic regions. Vicinity of the O1 atoms are indicated by black circles while O2 atoms are located with two different colors (white circles for Ob and grey circles for Oc). EP is around -0.485 e.Å^{-1} (green color) for all the atom of tha anion, while EP at the molecular surface takes different values for O2 from -0.537 e.Å^{-1} (red color, in the vicinty of Ob) to -0.485 e.Å^{-1} (green color, in the vicinty of Oc). The EP value at the molecular surface seems sensitive to the two bridging oxygen atom types (Ob and Oc) position, while the absolute difference is small (0.05 e.Å^{-1}). Lopez *et al* [34] has shown that the most effectively solvated site by H_2O molecules is the terminal oxygen (O1) because, although it carries the lowest negative charge, it is the most external. On the other hand, the bridging oxygens Ob, the most internal ones, are poorly solvated [34]. Chen *et al* [87]have very earlier determined the theoretical EP of WPA^{3-} anion and published it in a 2D representation but the quality doesnot allow a significant comparison. Additionally, these results can be compared to those obtained for two other POM compounds $[V_{10}O_{28}]^{6-}$ [84, 86] and functionalized hexavanadate [88]. In all cases the bridged atoms are more reactive than the terminal one. The two other studies where the EP values is mapped on a molecular surface for $[\{Zr(O_2)(\alpha\text{-}SiW_{11}O_{39})\}_2]^{12-}$ [89] and for $[HPTi(O_2)W_{11}O_{39}]$ [90], donot allow a discrimination between the different oxygen atoms.

One have to noticed than, due to the precision of the classical X-ray structures, we have decided not to discriminate between the two types of O2 oxygen atoms. However, the sensibility of the theoretical calculations allow us to see a difference in term of electrostatic potential. An analysis of the MEP indicates that, on one hand, the bridging O sites should be the most favorable for a protonation and, on the other, that the terminal oxygen is not a good position for protonation. But, the terminal oxygen (O1), although it carries the lowest negative charge, is the most external and interacts strongly *via* hydrogen bonds with organic moieties. Similarly, analysis of interactions in solid state show that Keggin anion

interacts very strongly with positively charged proteins *via* hydrogen bonds and that both O1 and O2 atoms are involved in non-covalent interactions. However O1 atom builds the strongest interactions.Therefore this study shows that the negatively charged Keggin anion interact very strongly with positively charged protein. Biological activities and reactivity mechanism is a competition between charges and accessibility. Reactivity of Keggin anion with proteins offers unique insight into their exact binding mode at the molecular level and may advance the application of POMs as a new class of proteases. This interesting reactivity has been illustrated and demonstrated through the following by NMR of Na+/K+-ATPase inhibition.We found indication of the enzyme interaction with a monolacunary WPA anion by 31P NMR spectrometry as presented in Fig. 4b. Therefore statistical crystallographic analysis and theoretical of various interactions of WPA, has been provided (PDB, EP and DFT), with an emphasis on the changes of bonding nature depending on the oxygen position in the molecules of WPA (O1 or O2).

4. Conclusion

The obtained results of ^{31}P NMR spectroscopy confirm that WPA exhibits inhibitory effect on the activity of Na+/K+-ATPase. Electrostatic effect and hydrogen bond interactions contribute to the enzyme (ATPase) – inhibitor (WPA) complex formation. In the solid state, the systematic description and interpretation of non-covalent interactions show that WPA interacts very strongly with protein *via* hydrogen bonds. Both O1 and O2 atoms are involved in non-covalent interactions but O1 atom builds the strongest interactions. The data retrieved from PDB showed that WPA interacts with the positively charged protein regions *via* hydrogen bonds.We confirm from *ab initio* calculations (Bader charges and EP on the molecular surface of WPA) that bridging oxygen (O2) are generally more basic than terminal oxygen.As a result, WPA *via* hydrogen bond should form relative stable complex with protein receptors.

Acknowledgements

ZY thanks Chinese Science Council for scholarship. NBP thanks CentraleSupelec for invited associated professor position. NBP, DBB, JZ and IHA would like to thank the Ministry of Education, Science and Technological Development of the Republic of Serbia for financial support (Project No OI 172043).

Supporting information

References of the structures retrieved from the four different bases are given as supporting information.

Abbreviations

ADP - adenosine diphosphate

AIM - Atoms in Molecules

AMP - adenosine monophosphate

ATP - adenosine triphosphate

COD – Crystallographic Open Database

CSD - Cambridge Structural Database

DFT - density functional theory

E-NTPDase - ecto-nucleoside triphosphate diphosphohydrolase

EP - Electrostatic potential

FTIR - Fourier Transform Infra Red spectroscopy

HIV - Human immunodeficiency virus

ICSD - Inorganic Crystal Structure Database

NMR - Nuclear magnetic resonance

PDB - Protein Data Bank

Pi - inorganic phosphate

POMs - Polyoxometalates

REDOR - Rotational Echo Double Resonance

WPA - 12-tungstophosphoric acid$H_3PW_{12}O_{40}$

References

1. M.T. Pope, A. Müller, Polyoxometalate Chemistry: From Topology via Self-Assembly to Applications, Kluwer: Dordrecht-Boston-London, (**2001**).
2. I.V. Kozhevnikov, Advances in Catalysis by Heteropolyacids, *Russ. Chem. Rev.*56 (**1987**) 811-825.
3. T. Okuhara, N. Mizuno, M. Misono, Catalytic Chemistry of Heteropoly Compounds, *Adv. Catal.*41 (**1996**) 113-252.
4. M. Misono, C.R. Misono, Acid catalysts for clean production. Green aspects of heteropolyacid catalysts, *Acad Sci Paris Serie II Chim Chem*3 (**2000**) 471-475.
5. M. Misono,Unique acid catalysis of heteropolycompounds(heteropolyoxometalates) in the solid state, *Chem. Commun.*(**2001**) 1141-1152.
6. M.T. Pope, A. Muller, Polyoxometalate chemistry - an old field with new dimensions in several disciplines, *Angew Chem.* 30 (**1991**) 34-48.
7. M.T. Pope, A. Muller (Ed), Polyoxometalates: from Platonic solids to Anti Retroviral Activity, Kluwer, Dordrecht, (**1994**).
8. J.T. Rhule, C.L. Hill, D.A. Judd, R.F. Schinazi, Polyoxometalates in Medicine. *Chem. Rev.*98 (**1998**) 327-357.
9. B. Hasenknopf, Polyoxometalates introduction to a class of inorganic compounds and their biomedical applications, *Front. Biosci.*10 (**2005**) 275-287.
10. A. Bijelić, A. Rompel, The use of polyoxometalates in protein crystallography – An attempt to widen a well-known bottleneck, *Coord. Chem. Rev.* 299 (**2015**) 22-38.

11. T. Yamase, H. Fujita, K. Fukushima, Medical chemistry of polyoxometalates. Part 1. Potent antitumor activity of polyoxomolybdates on animal transplantable tumors and human cancer xenograft, *Inorg. Chim. Acta* 151 (**1988**) 15-18.

12. T. Yamase, H. Fujita, K. Fukushima, T. Sakurai, Anticancer agents containing heteropolytungstates, *Jpn. Kokai Tokkyo Koho*, Terumo Corp., Japan, Jp 02204415 (**1990**).

13. T. Yamase, H. Fujita, K. Fukushima, T. Sakurai, Heteropolyacid salts as antitumor agents, *Jpn. Kokai Tokkyo Koho*, Terumo Corp., Japan, Jp 02088524 (**1990**).

14. J.F Liu,Y.G. Chen, L. Meng, J. Guo, Y. Liu, M.T. Pope, Synthesis and characterization of novel heteropoly-tungstoarsenates containing lanthanides $[LnAs_4W_{40}O_{140}]^{25-}$ and their biological activity, *Polyhedron* 17 (**1998**) 1541-1546.

15. X. Wang, J. Liu, M.T. Pope, New polyoxometalate/starch nanomaterial: synthesis, characterization and antitumoral activity, *Dalton Trans.*(**2003**) 957-960.

16. F. Bussereau, M. Picard, J. Blancou, P. Sureau, Treatment of rabies in mice and foxes with antiviral compounds, *Acta Virol.* 32 (**1988**) 33-49.

17. D.A. Judd, J.H. Nettles, N. Nevins, J.P. Snyder, D.C. Liotta, J. Tang, J. Ermolieff, R.F. Schinazi, C.L. Hill, Polyoxometalate HIV-1 protease inhibitors. A new mode of protease inhibition, *J. Am. Chem. Soc.* 123 (**2001**) 886-897.

18. N. Fukuda, T. Yamase, Y. Tajima, Inhibitory effect of polyoxotungstates on the production of penicillin-binding proteins and beta-lactamase against methicillin-resistant Staphylococcus aureus, *Biol. Pharm. Bull.*22(**1999**) 463-470.

19. X.H Wang,J.F. Liu, Y.G. Chen, Q. Liu, J.T. Liu, M.T. Pope, Synthesis, characterization and biological activity of organotitanium substituted heteropolytungstates, *Dalton Trans. A*-(**2000**) 1139-1142.

20. G. Zhang, B. Keita, C.T. Craescu, S. Miron, P. deOliveira, L. Nadjo, Polyoxometalate Bindingto Human Serum Albumin: A Thermodynamic and Spectroscopic Approach, *J. Phys. Chem. B.* 111 (38) (**2007**) 11253-11259.

21. Y. Zhou, L. Zheng, F. Han, G. Zhang, Y. Ma, J. Yao, B. Keita, P. de Oliveira, L. Nadjo, Inhibition of amyloid-β protein fibrillization upon interaction with polyoxometalates nanoclusters, *Colloids Surf. A-Physicochem. Eng. Asp.* 375 (**2011**) 97-101.

22. R.J. Russell, L.F. Haire, D.J. Stevens, P.J. Collins, Y.P. Lin, G.M. Blackburn, A.J. Hay, S.J. Gamblin, J.J. Skehel, The structure of H5N1 avian influenza neuraminidase suggests new opportunities for drug design, *Nature* 443 (**2006**) 45-49.

23.G. Zhang,B. Keita,J.C Brochon, P. de Oliveira,L. Nadjo, C. T. Craescu, S. Miron, Molecular Interaction and Energy Transfer between Human Serum Albumin and Polyoxometalates, *J. Phys. Chem. B.*111(7) (**2007**) 1809–1814.

24. C. Baroi, Ajay K. Dalai, Review on Biodiesel Production from Various Feedstocks Using 12-Tungstophosphoric Acid (TPA) as a Solid Acid Catalyst Precursor, *Ind. Eng. Chem. Res.*53 (**2014**) 18611-18624.

25. G. Marci, EI Garcia-Lopez, L. Palmisano, Heteropolyacid-Based Materials as Heterogeneous Photocatalysts, *Eur. J. Inorg. Chem.* 1 (**2014**) 21-35.

26. V.S. Kuntić, I.M. Filipović, U.B. Mioč, S.B. Jelić, Anticoagulant effect of various crystallohydrates of tungstophosphoric acid and their Na salt and proposed acting mechanism, J*ugoslav. Med. Biohemija-Yugoslav Med. Biochem*. 16(1) (**1997**) 15-19.

27. Y. Wang, S. Liu, Z. Liu, J. Yang, X. Hu, Study on the interactions of antiemetic drugs and 12-tungstophosphoric acid by absorption and resonance Rayleigh scattering spectra and their analytical applications, *Spectroc. Acta Pt. A-Molec. Biomolec. Spectr.* 15(105) (**2005**) 612-617.

28. S. Uskoković-Marković, M. Milenković, A. Topić, J. Kotur-Stevuljević, A. Stefanović, J. Antić-Stanković, Protective Effect of Tungstophosphoric Acid and Sodium Tungstate on Chemically Induced Liver Necrosis in Wistar Rats, *J. Pharm. Pharm. Sci.* 10(3) (**2007**) 340-349.

29. A. Topić, M. Milenković, S. Uskoković-Marković, D. Vucicević, Insulin mimetic effect of tungsten compounds on isolated rat adipocytes, *Biol. Trace Elem. Res.* 134(3) (**2010**) 296-306.

30. C. Li, X. Hu, S. Liu, Z. Liu, Study on the interaction between torasemide and 12-tungstophosphoric acid by resonance Rayleigh scattering and resonance nonlinear scattering spectra and its analytical applications, *Spectroc. Acta Pt. A-Molec. Biomolec. Spectr.* 79(5) (**2011**) 1084-1090.

31. M. Čolović, D. Bajuk-Bogdanović, N. Avramović, I. Holclajtner-Antunović, N. Bošnjaković-Pavlović, V. Vasić, D. Krstić, Inhibition of rat synaptic membrane Na+/K+-ATPase and ecto-nucleoside triphosphate diphosphohydrolases by 12-tungstosilicic and 12-tungstophosphoric acid, *Bioorg. Med. Chem.* 19 (**2011**) 7063–7069

32. P. Pavli, P.S. Petrou, A.M. Douvas, D, Dimotikali, S.E. Kakabakos, P. Argitis, Protein-resistant cross-linked poly(vinyl alcohol) micropatterns via photolithography using removable polyoxometalate photocatalyst, *ACS Appl. Mater. Interfaces*, 6(20) (**2014**) 17463-17473.

33. Y. Zhang, D. Zhang, J. Zhang, Y. Zhang,L. Liu, X. Zhang, Y. Feng, J. Sha, Y. Zhang, C. Wang, Y. Shen, H. Kuang, Synthesis, characterization and antibacterial properties of two POM-based supramolecular compounds with the natural activeingredient: $(THB)_3(H_5PMo_{12}O_{40})$ and $(THB)_3(H_3PW_{12}O_{40})$, *Inorg. Chem. Commun.* 74 (**2016**) 6-11.

34. X. Lopez, C. Nieto-Draghi, C. Bo, J. Bonet Avalos, J.M. Poblet, Polyoxometalates in Solution: Molecular Dynamics Simulations on the α-$PW_{12}O_{40}^{3-}$ Keggin Anion in Aqueous Media, *J. Phys. Chem. A* 109, (**2005**) 1216-1222.

35. I.V. Kozhevnikov, A. Sinnema, H. Bekkum,Proton sites in Keggin heteropoly acids from^{17}O NMR,*Catal. Lett.* 34 (**1995**) 213-221.

36. S. Ganapathy, M.Fournier, J.F. Paul, L. Delevoye, M. Guelton, J.P. Amoureux, Location of Protons in Anhydrous Keggin Heteropolyacids $H_3PMo_{12}O_{40}$ and $H_3PW_{12}O_{40}$ by $^{1}H\{^{31}P\}$/ $^{31}P\{^{1}H\}$ REDOR NMR and DFT Quantum Chemical Calculations,*J. Am. Chem. Soc.* 124 (**2002**) 7821-7828.

37. S.J. Huang, C.Y. Yang, A. Zheng, N. Feng, N. Yu, P.H. Wu, Y.C. Chang, Y.C. Lin, F. Deng, S.B. Liu, New Insights int oKeggin-Type 12-TungstophosphoricAcid from ^{31}P MAS NMR Analysis of Absorbed Trimethylphosphine Oxide and DFT Calculations, *Chem.-Asian J.* 6 (**2011**) 137-148.

38.T. Ueda, T. Tatsumi, T. Eguchi, N.J. Nakamura, Structure and properties of acidic protons in anhydrous dodecatungstophosphoric acid, $H_3PW_{12}O_{40}$, as studied by solid-state H-^{1}, H-^{2}NMR, and H-^{1}-P-^{31}SEDORNMR, *J. Phys. Chem. B* 105 (**2001**) 5391-5396.

39.B.B. Bardin, S.V. Bordawekar, M. Neurock, R.J. Davis, Acidity of Keggin-Type Heteropolycompounds Evaluated by Catalytic Probe Reactions, Sorption Microcalorimetry, and Density Functional Quantum Chemical Calculations,*J. Phys. Chem. B* 102 (**1998**) 10817-10825.

40. M. J. Janik, K. A.Campbell, B. B.Bardin, R.J. Davis, M. Neurock, A computational and experimental study of anhydrousphosphotungstic acid and its interaction with water molecules, Neurock, *Appl. Catal. A-Gen.* 256 (**2003**) 51-68.

41.J. Yang, M.J. Janik, D. Ma, A. Zheng, M. Zhang, M. Neurock, R.J. Davis, C. Ye, F. Deng, Location, Acid Strength, and Mobility of the Acidic Protonsin Keggin 12-$H_3PW_{12}O_{40}$: A Combined Solid-State NMR Spectroscopy and DFT Quantum Chemical Calculation, *J. Am. Chem. Soc.* 127 (**2005**) 18274-18280.

42. T.R. Brown, K. Ugurbil, R.G. Shulman, ^{31}P nuclear magnetic resonance measurements of ATPase kinetics in aerobic Escherichiacoli cells, *Proc. Natl. Acad. Sci. U. S. A.* 74 (**1977**) 5551-5553.

43. B.D.N. Rao, M. Cohn, Asymmetric binding of the inhibitor di(adenosine-5') pentaphosphate (Ap5A) to adenylate kinase, *Proc. Natl. Acad. Sci. U. S. A.*. 74 (**1977**) 5355-5357.

44. M.Cohn, B.D.N. Rao,^{31}P NMR studies of enzymatic reactions, *Bulletin of Magnetic Resonance*, 1(1) (**1979**) 38-60.

45. M. Cohn, T.R. Hughes, Phosphorus magnetic resonance spectra of adenosine diphosphate and triphosphate. 1. Effect of pH, *J. Biol. Chem.* 235(11) (**1960**) 3250-3253.

46. F.H. Allen, The Cambridge Structural Database: a quarter of a million crystal structures and rising, *Acta Crystallogr.* B58 (**2002**) 380-388.

47. S. Gražulis, A. Daškevič, A. Merkys, D. Chateigner, L. Lutterotti, M. Quirós, N.R. Serebryanaya, P. Moeck, R.T Downs, A. LeBail, Crystallography Open Database (COD): an open-access collection of crystal structures and platform for world-wide collaboration, *Nucleic Acids Res.*40, (**2012**) D420-D427.

48. CSD, Karlsruhe, Fachinformationszentrum (FIZ) Karlsruhe (**2007**).

49. H.M. Berman, J. Westbrook, Z. Feng, G. Gilliland, T.N. Bhat, H. Weissig, I.N. Shindyalov, P.E. Bourne, The Protein Data Bank, *Nucleic Acids Res.* 28 (**2000**) 235-242.

50. G.Bogdanović, A. Spasojević-de Biré, S. Zarić, Evidence of a C-H···π interaction between an organic moiety and a chelate ring in transition metal complexes based on crystal structures and computations, *Eur. J. Inorg. Chem.*(**2002**) 1599-1602.

51. O. Takahashi, Y. Kohno, M. Nishio, Evidence from Recent Experimental Data and High-Level ab Initio MO Calculations, *Chem. Rev.* 110 (**2010**) 6049-607.

52.A.J. Cruz-Cabeza, S.M. Reutzel-Edens, J. Bernstein, Facts and fictions about polymorphism, *Chem. Soc. Rev.* 44(23) (**2015**) 8619-8635.

53. K. Takiededdin, Y. Z. Khimyak, L. Fabian, Prediction of Hydrate and Solvate Formation Using Statistical Models, *Cryst. Growth Des.*16(1) (**2016**) 70-81.

54. N. Bošnjaković-Pavlović, J. Prevost, A. Spasojević-de Biré, Crystallographic Statistical Study of Decavanadate Anion Based-Structures: Toward a Prediction of Noncovalent Interactions, *Cryst. Growth Des.* 11 (**2011**) 3778-3789.

55. X. Xu,N. Bošnjaković-Pavlović,M.B.Čolović,D.Z.Krstić, V.M. Vasić, J.M. Gillet,P. Wu, Y. Wei, A. Spasojević-de Biré, A combined crystallographic analysis and *ab initio* calculations to interpret the reactivity of functionalized hexavanadates and their inhibitor potency toward Na^+/K^+-ATPase, *J. Inorg. Biochem.*161 (**2016)** 27-36.

56. G. Brauer, Handbuch der Präparativen Anorganischen Chemie, Ferdinand Enke Verlag, Stuttgart, (**1981**)

57. C.F. Macrae, I.J. Bruno, J.A. Chisholm, P.R. Edgington, P. McCabe, E. Pidcock, L. Rodriguez-Monge, R. Taylor, J. van de Streek, P.A. Wood, Mercury CSD 2.0 - New Features for the Visualization and Investigation of Crystal Structures, *J. Appl. Cryst.* 41 (**2008**) 466-470

58. M. J. Frisch, G. W. Trucks, H. B. Schlegel, G. E. Scuseria, M. A. Robb, J. R. Cheeseman, G. Scalmani, V. Barone, G. A. Petersson, H. Nakatsuji, X. Li, M. Caricato, A. Marenich, J. Bloino, B. G. Janesko, R. Gomperts, B. Mennucci, H. P.

Hratchian, J. V. Ortiz, A. F. Izmaylov, J. L. Sonnenberg, D. Williams-Young, F. Ding, F. Lipparini, F. Egidi, J. Goings, B. Peng, A. Petrone, T. Henderson, D. Ranasinghe, V. G. Zakrzewski, J. Gao, N. Rega, G. Zheng, W. Liang, M. Hada, M. Ehara, K. Toyota, R. Fukuda, J. Hasegawa, M. Ishida, T. Nakajima, Y. Honda, O. Kitao, H. Nakai, T. Vreven, K. Throssell, J. A. Montgomery, Jr., J. E. Peralta, F. Ogliaro, M. Bearpark, J. J. Heyd, E. Brothers, K. N. Kudin, V. N. Staroverov, T. Keith, R. Kobayashi, J. Normand, K. Raghavachari, A. Rendell, J. C. Burant, S. S. Iyengar, J. Tomasi, M. Cossi, J. M. Millam, M. Klene, C. Adamo, R. Cammi, J. W. Ochterski, R. L. Martin, K. Morokuma, O. Farkas, J. B. Foresman, and D. J. Fox, "Gaussian 09, Revision A.02", Gaussian, Inc., Wallingford CT, (**2016**)

59. A.D. Becke, Density-functional exchange-energy approximation with correct asymptotic behavior, *Phys.Rev.A* 38(6) (**1988**) 3098-3100.

60. C. Lee, W.Yang, R.G. Parr, Development of the Colle-Salvetti correlation-energy formula into a functional of the electron density, *Phys.Rev. B* 37(2) (**1988**) 785-789.

61. B. Miehlich, A. Savin, H. Stoll, H. Preuss, Results obtained with the correlation energy density functionals of Becke and Lee, Yang and Parr, *Chem. Phys. Lett.* 157(3) (**1989**) 200-206.

62. R.A. Kendall, T.H. Dunning, R.J. Harrison, Electron affinities of the first-row atoms revisited. Systematic basis sets and wave functions, *J. Chem. Phys.* 96(9) (**1992**) 6796-6806.

63. P.J Hay, W.R. Wadt. Ab initio effective core potentials for molecular calculations. Potentials for the transition metal atoms Sc to Hg, *J. Chem. Phys.* 82(1) (**1985**) 270-283.

64. D. Marvin, N.M.M. Kroll. Quantum electrodynamical corrections to the fine structure of helium. *Ann. Phys.* 82(1) (**1974**) 89-155.

65. B.A. Hess, Relativistic electronic-structure calculations employing a two-component no-pair formalism with external-field projection operators, *Phys. Rev. A* 33(6) (**1986**) 3742-3748.

66. T. Lu, F. Chen, Multiwfn: A multifunctional wavefunction analyzer, *J. Comp. Chem.* 33 (**2012**) 580-592.

67. R.F.W. Bader, Atomsinmolecules. JohnWiley&Sons, Ltd, (**1990**).

68. I. Holclajtner-Antunović, D. Bajuk-Bogdanović, M. Todorović, U. Mioč, J. Zakrzewska, S. Uskoković-Marković, Spectroscopic study of stability and molecular species of 12-tungstophosphoric acid in aqueous solution, *Can. J. Chem.* 86 (**2008**) 996-1004.

69. B.J. Smith, V.A. Patrick, Quantitative Determination of Aqueous Dodecatungsto-phosphoric Acid Speciation by NMR Spectroscopy, *Aust. J. Chem.* 57(3) (**2004**) 26-268.

70. K.N. Luong, P. Shestakova, G. Absillis, T.N. Parac-Vogt,Detailed Mechanism of Phosphoanhydride Bond Hydrolysis Promoted by a Binuclear Zr^{IV}-Substituted Keggin Polyoxometalate Elucidated by a Combination of ^{31}P, ^{31}P DOSY, and ^{31}P EXSY NMR Spectroscopy, *Inorg. Chem.*55 (10) (**2016**) 4864-4873.

71. P.J. Cozzone, O. Jardetzky,Phosphorus-31 fourier transform, nuclear magnetic resonance study of mononucleotides and dinucleotides. 1. Chemical shifts, *Biochemistry* 15 (**1976**) 4853-4863.

72. F.E. Evans, N.O. Kaplan, ^{31}P nuclear magnetic resonance studies of HeLa cells, *Proc. Natl. Acad. Sci. U. S. A.* 74 (**1977**) 4909-4913.

73. G. Desiraju, T.Steiner, The weak hydrogen bond: in structural chemistry and biology, International Union of Crystallography Monographs in Crystallography, 9, (**2001**).

74. P. Song, L.K. Yan, W. Guan, J.D. Feng, C.G. Liu, Z.M. Su,The comparative investigation on redox property and second-order nonlinear response of Keggin-type α-$[PM_{12}O_{39}NPh]^{3-}$ (M = W and Mo) and Mo_6NPh,*Chin. Sci. Bull.*54 (**2009**) 203-211.

75. Y. Zhou,J. Yang,H. Su, J. Zeng, S.P. Jiang, W.A. Goddard, Insight into Proton Transfer in Phosphotungstic Acid FunctionalizedMesoporous Silica-Based Proton Exchange Membrane Fuel Cells, *J. Am. Chem. Soc*. 136 (**2014**) 4954-4964.

76.R. Tokarz-Sobieraj, R. Grybos, U. Filek, A. Micek-Ilnicka, P. Niemiec, A. Kirpsza, M. WitkoJerzy, Generation of acidic sites in Al, Ga, In salts of molybdenumand tungsten Keggin-type heteropolyacids. DFT modelingand catalytic tests, *Catal. Today* 257 (**2015**) 72-79.

77. W. Guan, L. Yan, Z. Su, S. Liu, M. Zhang, X. Wang, Electronic Properties and Stability of Dititanium^{IV} Substituted α-Keggin Polyoxotungstate with Heteroatom Phosphorus by DFT, *Inorg. Chem.* 44 (1) (**2005**) 100-107.

78. Y.R. Guo, Q.J. Pan, Y.D. Wei, Z.H. Li, X. Li, Theoretical studies on the electronic and spectroscopic propertiesof Keggin-structure polyoxometalates $[XM_{12}O_{40}]^{n-}$(X=Si, P; M=Mo, W), *J. Mol. Struct. (Theochem)* 676 (**2004**) 55-64

79. S.J. Huang, C.Y. Yang, A. Zheng, N. Feng, N. Yu, P.H. Wu, Y.C. Chang, Y-C. Lin, F. Deng, S.-B Liu, New Insights into Keggin-Type 12-Tungstophosphoric Acid from ^{31}P MASNMR Analysis of Absorbed Trimethylphosphine Oxide and DFTCalculations, *Chem. -Asian J*. 6 (**2011**) 137-148.

80. A.Chaumont, G. Wipff, Interactions between Keggin Anions in Water: The Higher Their Charge, the Higher Their Condensation? ASimulation Study, *Eur. J. Inorg. Chem.* (**2013**) 1835-1853.

81. D. Hu, C. Shao, W. Guan, Z. Su, J. Sun, Studies on the interactions of Ti-containing polyoxometalates (POMs) with SARS-CoV 3CLpro by molecular modeling, *J. Inorg. Biochem*. 101 (**2007**) 89-94.

82. J.P. Wang, D. H. Hu, Z. M. Su, Molecular simulation study of the binding mechanism of$[\alpha\text{-}PTi_2W_{10}O_{40}]^{7-}$ for its promising broad-spectrum inhibitoryactivity to FluV-A neuraminidase, *Chin. Sci. Bull* 55 (23) (**2010**) 2497-2504.

83. H. Wu, J. Wang, H. Li, N. Ma, T. Zhang, S. Shi, L. Yan, Z. Su Structure and Frontier Molecular Orbital (FMO) energies of a-Keggin-type polyoxometalate $[PW_{12}O_{40}]^{3-}$: A systematical study with different functionals of density functional theory, *Comput. Theor. Chem.* 1089 (**2016**) 28-34.

84. N. Bošnjaković-Pavlović, A. Spasojević-de Biré, I.Tomaz,N. Bouhmaida, F. Avecilla, U. Mio**č**, J. Costa Pessoa, N.E. Ghermani, Electron and electrosratiti properties oa a cytosine decavanadate compound from high resoultion x-ray diffraction: toward a better understanding of chemical and bilogical properties of decavadanadates, *Inorg. Chem*. 48 (20) (**2009)** 9742-9753.

85. M. Henry, Quantitative modelization of hydrogen-bonding in polyoxometalate chemistry, *J. Cluster Sci.* 13 (**2002**) 437-458.

86. J.Y. Kempf, M.M. Rohmer, J.M. Poblet, C. Bo, M. Bénard, Relative Basicities of the Oxygen Sites in $[V_{10}O_{28}]^{6-}$. An analysis of the ab initio determined distributions of the electrostatic potential and of the Laplacian of charge density, *J. Am. Chem. Soc.* 114(**1992**) 1136-1146.

87. T.L. Chen, J. Ji, S.X. Xiao, T.X. Cai, G.S. Yan, The electronic-structure of keggin anion (pw12o40)3- and catalytic properties, *Int. J. Quantum Chem.* 44(6) (**1992**) 1015-1025

88. a) X. Xu, Experimental and theoretical charge density analysis of functionalized polyoxovanadates: toward a better understanding of chemical bonding and chemical reactivity, Ecole Centrale Paris, (**2015**) <NNT : 2015ECAP0026><tel-01181264>. b) Experimental Evidence of Charge Transfer in a Functional-ized Hexavanadate. A High Resolution X-ray Diffraction Study, X. Xu, A. Spasojević-de Biré, N-E Ghermani, Y. Wei, S. Novaković, N. Bošnjaković-Pavlović, P. Wu, *Phys. Chem. Chem. Phys.* 19 (**2017**) 18162-18166.

89. M. Carraro, N. Nsouli, H. Oelrich, A. Sartorel, A. Sorar, S.S. Mal, G. Scorrano, L. Walder, U. Kortz, M. Bonchio, Reactive ZrIV and HfIV Butterfly Peroxides on Polyoxometalate Surfaces:Bridging the Gap between Homogeneous and Heterogeneous Catalysis, *Chem. Eur. J*. 17 (**2011**) 8371-8378.

90. O.A. Kholdeeva, T.A. Trubitsina, R.I. Maksimovskaya, A.V. Golovin, W.A. Neiwert, B.A. Kolesov, X. Lopez,J.M. Poblet, First Isolated Active Titanium Peroxo Complex: Characterization andTheoretical Study, *Inorg. Chem*. 43 (7) (**2004**) 2284-2292.

Table captions

Table 1. List of WPA structures used in this paper retrieved from the ICSD, CSD, COD and PDB searches. Structures are ranked in pure inorganic compound, organic – inorganic hybrid or co-crystals compounds and proteins co-crystalized with WPA. Structures with coordinates available and R factor < 10 % are listed. Code refers to ICSD codes in case of inorganic structures, CSD refcodes or COD numbers in case of organic – inorganic hybride or co-crystals structures or PDB id in case of protein inorganic co-crystals.

Table 2. Hydrogen bonds between Keggin anion and protein from **2hhl**, **1n7d** and **5suq** structures. Distances d(D…O) ≤ 3.50 Å have been reported. ARG- arginine,ASN-asparagine, ASP- aspartic acid, LYS-lysine, ARG-arginine, HIS-Hystidine, PHE-phenylalanine, SER-serine, THR- threonine.

Table 3. Theoretical average atomic charge of WPA^{3-}: Bader charges (this work, column #3), Mulliken charges [34], [36], [75] *, natural charges [78], net charges, unprecised method [81], CHelpG [34]**. Experimental charges on $[V_{10}O_{28}]^{6-}$: [84] and theoretical charges on $[V_{10}O_{28}]^{6-}$: PACHA charges [85], Mulliken charges [86] and Bader [87]. All charges in (in e). Δ corresponds to the difference between the charges of the bridged O2 atoms *minus* the charge of the terminal O1 atom.

Figures captions

Figure 1. Chemical structure and atom labeling of WPA a) wireframe bond style b) oxygen octahedral representation.

Figure 2. ^{31}P NMR spectra of blank, control, and probe solution recorded immediately after preparation (a), 4 h (b), and 4 days after preparation of solution (c).

Figure 3. Influence of WPA on ATP hydrolysis monitored by time changes of β-ATP signal intensity in ^{31}P NMR spectra. The presented values represent normalized area of β-ATP signal (normalization was done on integrated area from +10 to –30 ppm) in blank, control and probe solution.

Figure 4. ^{31}P NMR spectra of WPA in solution: a) WPA in the incubation medium in the absence enzyme and ATP, b) WPA in the incubation medium in the presence of the enzyme (without ATP).

Figure 5. Distribution of the D-H..O angle (in °) *versus* the H…O distances (in Å) according to the oxygen atom type for each donor typeobtained from the ICSD database search. (O-H···O squares, N-H···O, circles and C-H···O triangles).

Figure 6. Distribution of the value of the H···O distances (in Å) and C-H···O angle (in °) interactions according to the oxygen atom type obtained from the CSD database search.

Figure 7. Number of C-H···O interactions as a functions of the H···O distances (in Å), according to the oxygen atom type (ICSD and CSD databases searches).

Figure 8. Theoretical electrostatic potential (e.Å^{-1}) of WPA^{3-} mapped on isodensity surface (0.007 e.Å^{-3}) in three orientations of the structure. Black circles in the vicinity of O1. For O2, two colors are used: white circles in the vicinity of Ob and grey circles in the vicinity of Oc.

Table 1

Chemical formula	Code	Reference
Inorganic or hybride organic-inorganig structures retrieved from the ICSD base		
C_{12} H_{36} Fe O_{46} P S_6 W_{12}	250528	S3a
C_9 H_{30} N_3 O_{40} P W_{12}	166878	S3b
C_6 H_{24} N_3 O_{40} P W_{12}	166877	S3b
C_{21} H_{49} N_7 O_{47} P Pr W_{12}	167536	S3c
C_{14} H_{42} O_{47} P S_7 W_{12} Y	167537	S3c
H_{21} Mg O_{50} P W_{12}	416173	S3d
H_{15} O_{46} P W_{12}	95621	S3e
H_{15} O_{46} P W_{12}	95622	S3e
$H_{4.5}$ $D_{10.5}$ O_{46} P W_{12}	95625	S3e
H_{15} O_{46} P W_{12}	95624	S3e
H_{45} O_{61} P W_{12}	1534	S3f
H_{15} O_{46} P W_{12}	904	S3g
H_{15} O_{46} P W_{12}	908	S3g
Organic – inorganic hybrid compounds or organic – inorganic co-crystals retrieved from CSD or COD base		
C_{24} H_{35} N_4 O_{49} P W_{12}	JUVZUX	S1a
C_6 H_{18} N_3 O_{44} P W_{12}	OQOFOR	S1b
C_{30} $H_{56.94}$ Bi_3 N_6 O_{72} P Na W_{12}	EQOFEX	S1c
C_{24} H_{46} Cl Cu_2 N_4 O_{56} P W_{12}	UJAVAE	S1d
C_{60} H_{63} N_3 O_{52} P W_{12}	IXUWIJ	33
C_{24} H_{45} N_6 O_{40} P W_{12}	CSLGXY	S1e
C_{26} H_{40} Cl Cu_4 N_{32} O_{40} P S_8 W_{12}	JOFKAS	S1f
C_{40} H_{30} Cl Cu_2 N_{12} O_{43} P S_4 W_{12}	NOKTIS	S1g
C_{30} H_{24} Ag_2 N_6 O_{40} P W_{12}	FOKKIB	S1h
C_{24} H_{45} N_6 O_{40} P W_{12}	HIDGEI	S1i
C_{36} H_{33} Cu_5 N_{30} O_{45} P W_{12}	LIBKAK	S1j
C_{24} H_{28} N_4 O_{50} P W_{12}	KIVPIQ	S1k
C_{16} H_{25} Ag_4 N_{12} O_{40} P W_{12}	DEZNED	S1l

C_8 H_{27} N_6 O_{46} P W_{12}	DEZNAS	S1l
C_{24} H_{39} Ni_2 N_4 O_{60} P W_{12}	LIQFOI	S1m
C_{60} H_{60} Ag_3 N_{10} O_{40} P W_{12}	BIQQOJ	S1n
C_{48} H_{32} Cl_3 Cu_{12} N_{40} O_{40} P W_{12}	DAWWAB	S1o
C_{36} H_{33} Cu_6 N_{30} O_{45} P W_{12}	DAWVUU	S1o
C_{28} H_{40} Ag_5 N_{24} O_{40} P W_{12}	VAYWEZ	S1p
C_{96} H_{204} N_3 O_{40} P W_{12}	ABIJIG	S1q
C_{19} H_{24} N_5 O_{40} P W_{12}	AXORUB	S1r
C_{90} H_{72} $Cu_{4.5}$ N_{18} O_{40} P W_{12}	ETAYEE	S1s
C_{12} H_{12} Cu_3 N_6 O_{40} P W_{12}	SEHSEE	S1t
C_{18} H_{24} Cu_3 N_6 P W_{12} O_{40}	SEHRIH	S1t
C_{15} H_{21} Cu_2 N_5 P W_{12} O_{40}	SEHRON	S1t
C_{12} H_{13} Ag_3 N_6 P W_{12} $O_{40.5}$	SEHSAA	S1t
C_{144} H_{120} Au_9 P_8 O_{40} P W_{12}	WEVZIH	S1u
C_{66} H_{81} N O_{58} P Na_3 W_{12}	LEBREQ	S1v
C_{128} H_{103} N_{16} O_{42} P W_{12}	QAJKOC	S1w
C_{13} H_{41} Ba N O_{49} P S_4 W_{12}	AVUWIX	S1x
C_{64} H_{144} N_4 O_{40} P W_{12}	BIGLIN	S1y
C_{68} H_{56} Cu_3 N_{14} O_{40} P W_{12}	EDORIY	S1z
C_{65} H_{68} $Ni_{2.5}$ N_{13} $O_{41.5}$ P W_{12}	WIXSIF	S1α
C_{19} H_{73} N_{12} $O_{113.50}$ P_2 W_{24}	2226573	S2a

Protein name	**PDB id**	**Reference**
Human CTD small phosphatase-like protein	2HHL	S4a
Human extracellular domain of the LDL-receptor	1N7D	S4b
Saccharomyces cerevisiae	5SUQ	S4c

Table 2.

	1n7d			2hhl			5suq		
	Oxygen type	**Amino acid**	**d(D…O) (Å)**	**Oxygen type**	**Amino acid**	**d(D…O) (Å)**	**Oxygen type**	**Amino acid**	**d(D…O) (Å)**
OH…O	O1	ASN	3.37				O1	THR	3.0
	O1	SER	3.05				O1	ASP	3.0
	O1	ARG	2.44						
NH…O				O2	HIS	2.46	O2	LYS	1.7
				O2	LYS	2.93	O1	ARG	1.7
				O1	PHE	3.25	O1	ASN	2.4
							O1	ASN	2.7
							O1	ARG	2.9
							O2	ARG	3.0
							O1	ARG	3.0
							O1	ARG	3.3
							O1	ARG	3.3
CH…O	O1	ARG	2.86	O1	PHE	2.52			
	O2	ARG	2.51	O1	SER	2.85			
	O1	ARG	3.08	O1	LYS	2.93			
	O2	ARG	3.26	O2	HIS	3.06			
	O2	ARG	3.48	O1	PHE	3.06			
				O2	LYS	3.08			
				O1	PHE	3.22			
				O1	PHE	3.25			
				O1	PHE	3.12			
				O2	LYS	3.32			

~

Table 3

Atom	**Atomic charge**	**Bader charge**	[35]	[82]	[80]	[85]	[91]*	[91]**	[88]	[89]	[90]	[93]
			$[PW_{12}O_{40}]^{3-}$						$[V_{10}O_{28}]^{6-}$			
W	70.82	3.18	2.70	2.23		2.37	2.49	3.81				
P	11.06	3.94		2.71			2.43	1.51				
O_{inner}	9.56	-1.56		-1.17								
O1	8.94	-0.94	-0.74	-0.60	-0.69	-0.69	-0.72	-0.85	<-0.64>	<-0.558>	<-0.64>	<-0.899>
O2	9.15	-1.158 -1.143	-1.00 -1.07	-0.87 -0.84	-0.90	-0.90	-0.93 -0.94	-1.37 -1.55	<-0.811>	<-0.675>	<-0.90>	<-1.040>
PO_4		-2,3		-1.97	-1.66	-1.66						
V									<1.561≥	<1.759>	<2.06>	<2.272>
Δ		-0.21	-0.26	-0.27	-0.21	-0.21	-0.21	-0.61	-0.171	-0.117	-0.26	-0.141

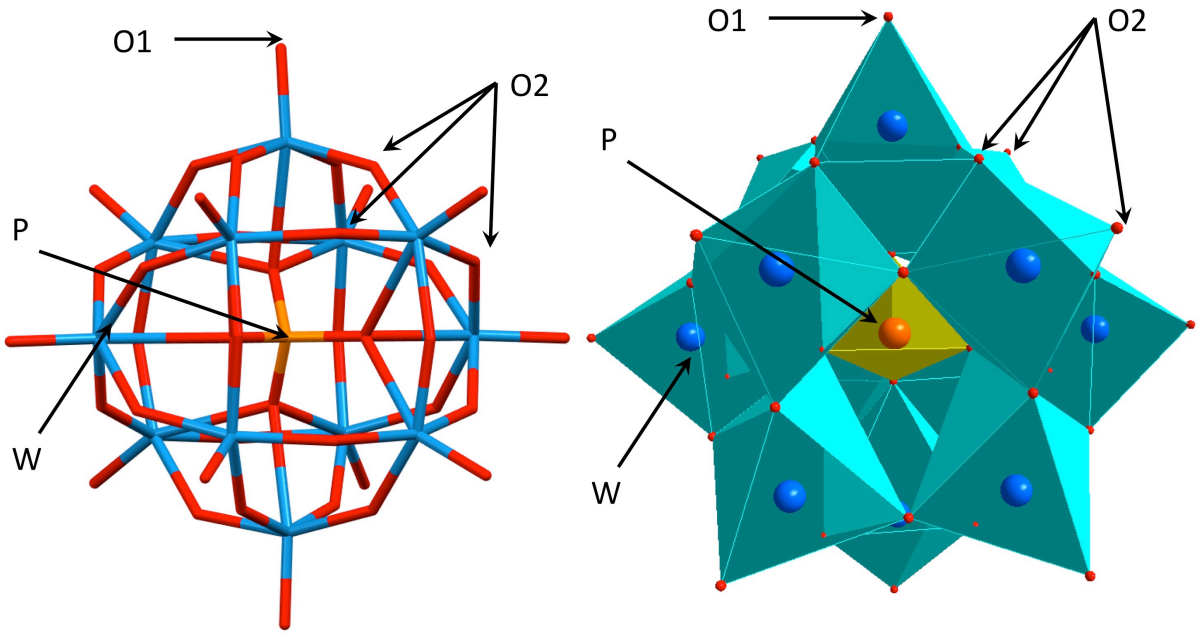

Figure 1.

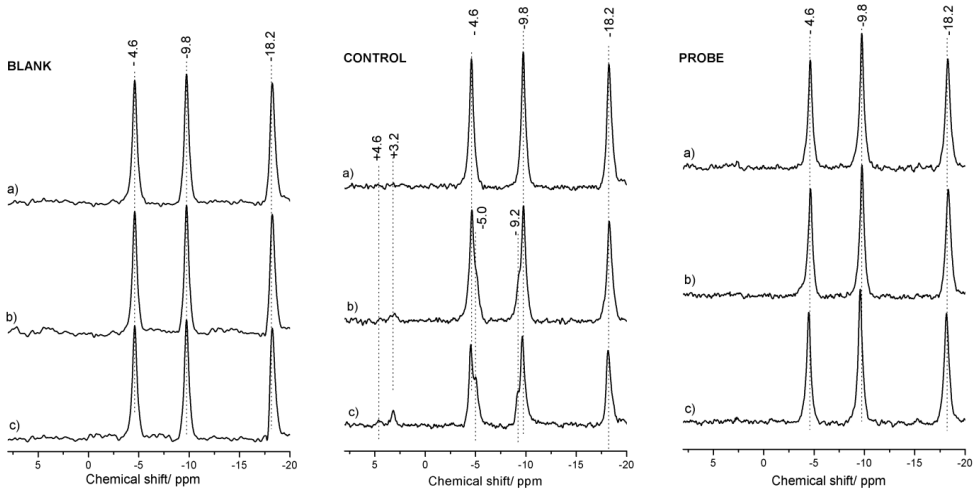
BLANK
-4.6
-9.8
-18.2
a)
b)
c)
5
0
-5
-10
-15
-20
Chemical shift/ ppm
CONTROL
-4.6
-9.8
-18.2
+4.6
+3.2
-5.0
-9.2
a)
b)
c)
5
0
-5
-10
-15
-20
Chemical shift/ ppm
PROBE
-4.6
-9.8
-18.2
a)
b)
c)
5
0
-5
-10
-15
-20
Chemical shift/ ppm

Figure 2.

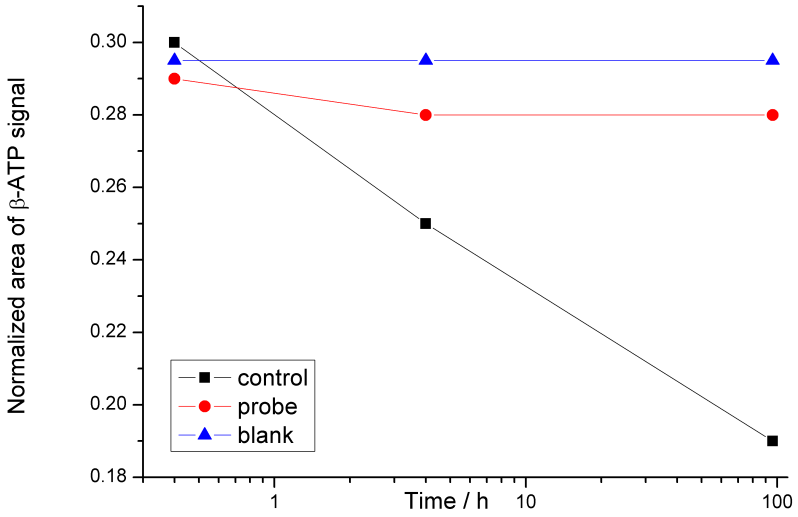
Normalized area of β-ATP signal
0.30
0.28
0.26
0.24
0.22
0.20
0.18
1
10
100
Time / h
control
probe
blank

Figure 3

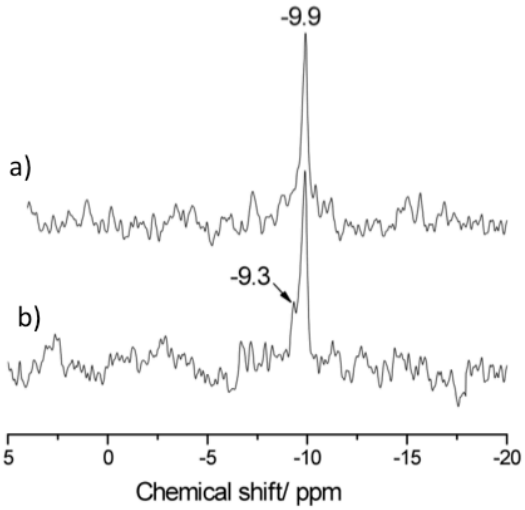

Figure 4

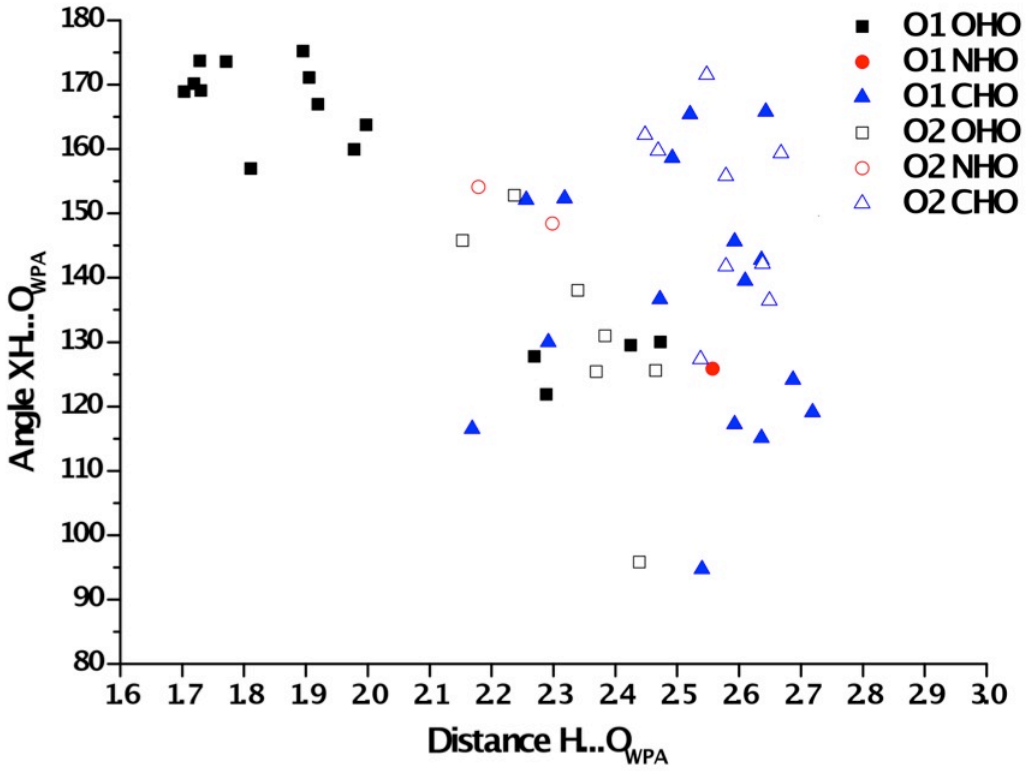
O1 OHO
O1 NHO
O1 CHO
O2 OHO
O2 NHO
O2 CHO
Angle XH...O_WPA
Distance H...O_WPA
180
170
160
150
140
130
120
110
100
90
80
1.6
1.7
1.8
1.9
2.0
2.1
2.2
2.3
2.4
2.5
2.6
2.7
2.8
2.9
3.0

Figure 5.

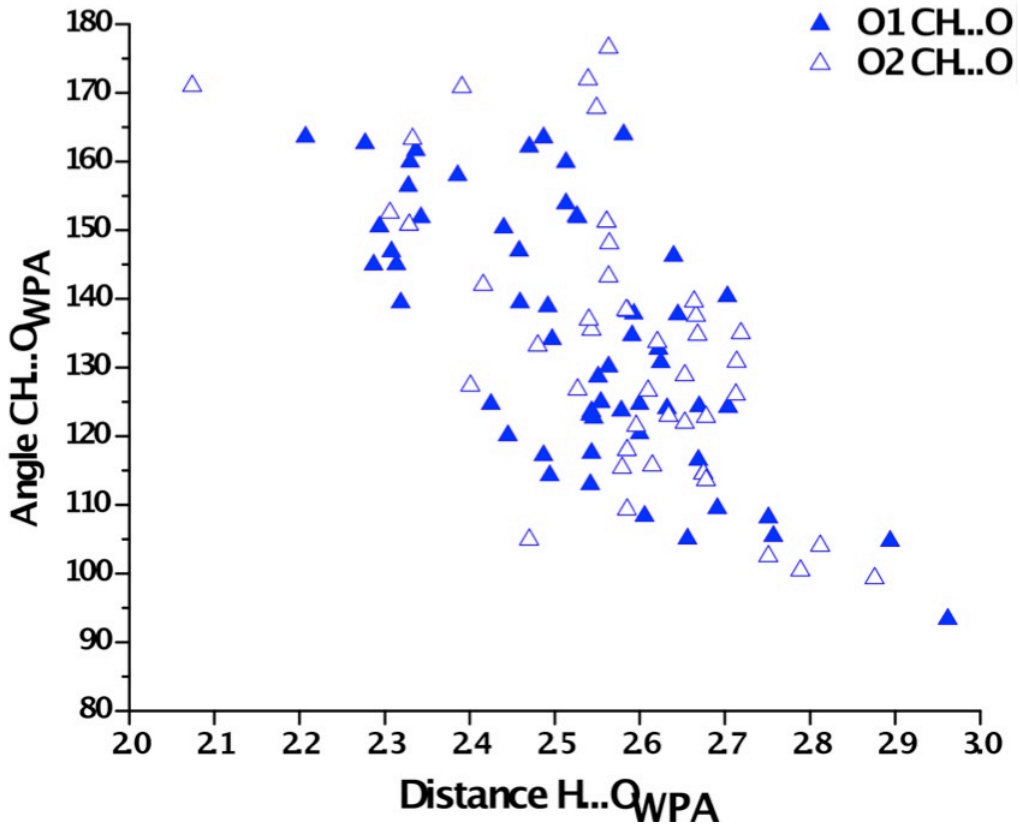
O1 CH...O
O2 CH...O
Angle CH...O_WPA
Distance H...O_WPA
180
170
160
150
140
130
120
110
100
90
80
20
21
22
23
24
25
26
27
28
29
30

Figure 6.

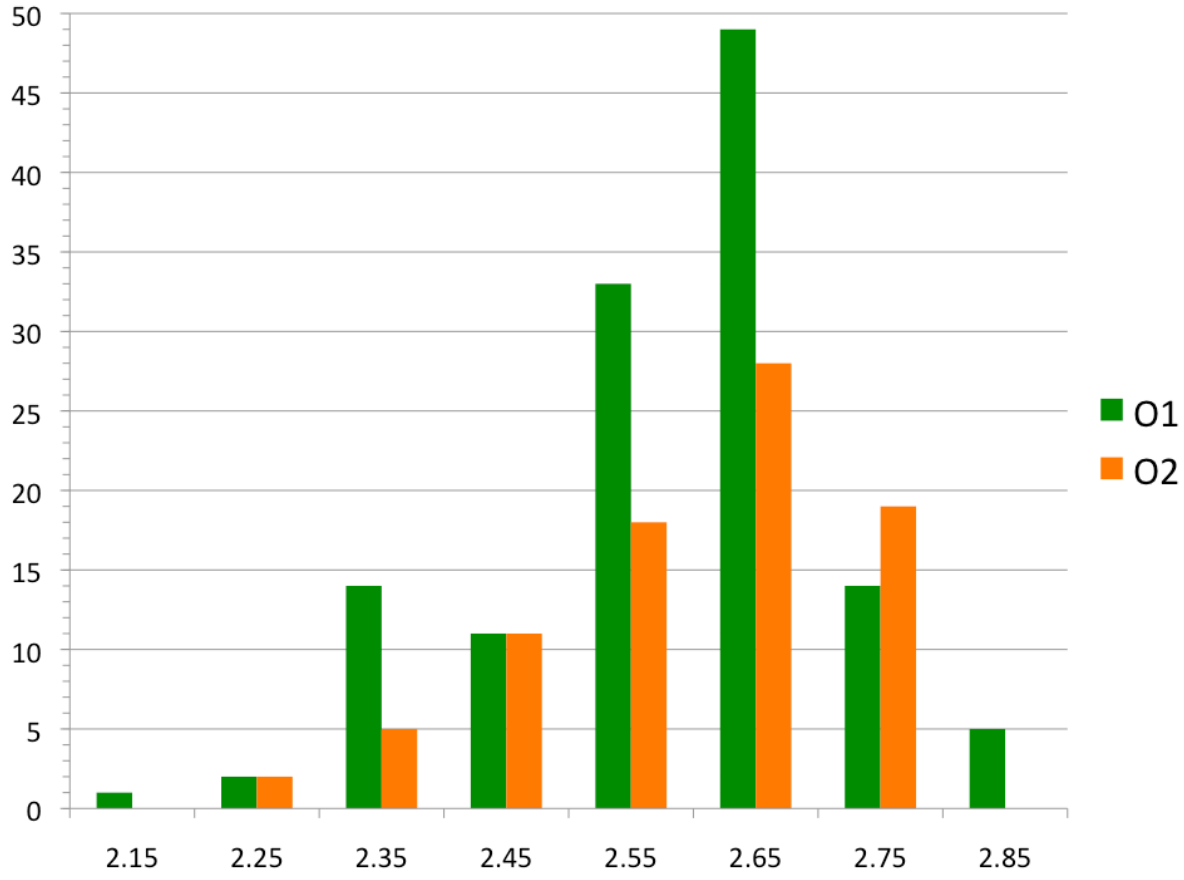

Figure 7.

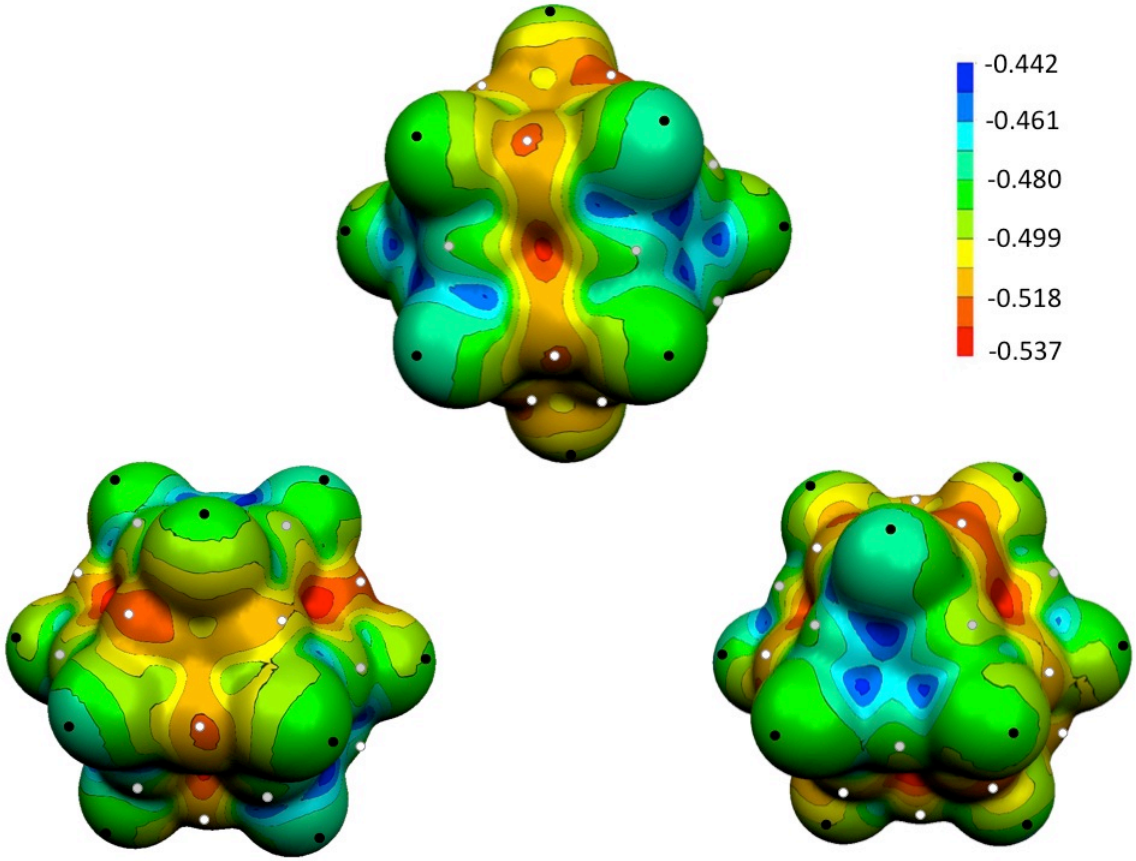

Figure 8.